MURDOCH RESEARCH REPOSITORY

This is the author's final version of the work, as accepted for publication following peer review but without the publisher's layout or pagination. The definitive version is available at
http://dx.doi.org/10.1099/vir.0.83676-0

Chua, B.H., Phuektes, P., Sanders, S.A., Nicholls, P.K. and McMinn, P.C. (2008) *The molecular basis of mouse adaptation by human enterovirus 71.* **Journal of General Virology, 89 (7). pp. 1622-1632.**

http://researchrepository.murdoch.edu.au/543/

The molecular basis of mouse adaptation by human enterovirus 71

Beng Hooi Chua[1],†, Patchara Phuektes[1,2],†, Sharon A. Sanders[1], Philip K. Nicholls[2] and Peter C. McMinn[1,3]

Abstract

A mouse-adapted strain of human enterovirus 71 (HEV71) was selected by serial passage of a HEV71 clinical isolate (HEV71-26M) in Chinese hamster ovary (CHO) cells (CHO-26M) and in newborn BALB/c mice (MP-26M). Despite improved growth in CHO cells, CHO-26M did not show increased virulence in newborn BALB/c mice compared with HEV71-26M. By contrast, infection of newborn mice with MP-26M resulted in severe disease of high mortality. Skeletal muscle was the primary site of replication in mice for both viruses. However, MP-26M infection induced severe necrotizing myositis, whereas CHO-26M infection caused only mild inflammation. MP-26M was also isolated from whole blood, heart, liver, spleen and brain of infected mice. CHO-26M harboured a single mutation within the open reading frame (ORF), resulting in an amino acid substitution of $K^{149} \rightarrow I$ in the VP2 capsid protein; two further ORF mutations that resulted in amino acid substitutions were identified in MP-26M, located within the VP1 capsid protein ($G^{145} \rightarrow E$) and the 2C protein ($K^{216} \rightarrow R$). Infectious cDNA clone-derived mutant virus populations containing the mutations identified in CHO-26M and MP-26M were generated in order to study the molecular basis of CHO cell and mouse adaptation. The VP2 ($K^{149} \rightarrow I$) change was responsible only for improved growth in CHO cells and did not lead to increased virulence in mice. Of the two amino acid substitutions identified in MP-26M, the VP1 ($G^{145} \rightarrow E$) mutation alone was sufficient to increase virulence in mice to the level observed in MP-26M-infected mice.

Introduction

Human enterovirus 71 (HEV71) belongs to the species *Human enterovirus A* of the genus *Enterovirus* within the family *Picornaviridae* (Stanway *et al.*, 2005). It is composed of a single-stranded, positive-sense RNA of approximately 7500 nt surrounded by an icosahedral capsid assembled from 60 copies of each of the four structural proteins, VP1, VP2, VP3 and VP4.

HEV71 was first isolated from an infant with encephalitis in California in 1969 (Schmidt *et al.*, 1974) and has since been associated with large outbreaks of hand, foot and mouth disease in young children, most recently in the Asia–Pacific region (Chumakov *et al.*, 1979; Lum *et al.*, 1998; McMinn *et al.*, 2001a). Although hand, foot and mouth disease is considered a mild febrile exanthem of childhood, HEV71 infection is associated with a high prevalence of

severe neurological disease, including aseptic meningitis, brainstem and/or cerebellar encephalitis and acute flaccid paralysis (reviewed by McMinn, 2002). With the almost successful eradication of poliomyelitis, HEV71 is now the leading cause of acute neurological infection in children of several Asian countries. Despite this, little is known about the pathogenesis of severe disease caused by HEV71.

Similar to the related poliovirus, HEV71 has a limited host range, with humans the only known natural host. Although Old World monkeys such as cynomolgus, rhesus and African green monkeys can be infected experimentally with HEV71 (Arita *et al.*, 2005; Chumakov *et al.*, 1979; Hashimoto & Hagiwara, 1982;Hashimoto *et al.*, 1978), other animal species, including rodents, are resistant to infection. Unfortunately, the high cost of monkeys and their maintenance precludes their widespread use for studies of viral pathogenesis. Thus, a small animal model would provide a more cost-effective and practical tool for studies of HEV71 pathogenesis and for vaccine development.

A recent study has reported the development of a mouse-adapted HEV71 strain (Chen *et al.*, 2004). Seven-day-old mice infected with mouse-adapted HEV71 by oral, intramuscular (i.m.), intraperitoneal (i.p.) or intracerebral (i.c.) inoculation developed acute flaccid paralysis mimicking HEV71 infection in humans and monkeys (Chen *et al.*, 2004; Wang *et al.*, 2004). Mouse-adapted HEV71 was more virulent in mice, exhibited a larger plaque size and grew more rapidly in cell culture than parental virus. Potential virulence determinants of this mouse-adapted strain were identified in the 5′-untranslated region (four nucleotide changes), the capsid protein VP2 (three nucleotide and one amino acid change) and the non-structural protein 2C (eight nucleotide and four amino acid changes) (Wang *et al.*, 2004). However, the role of these mutations in the virulence phenotype of the mouse-adapted strain was not determined.

In order to establish a mouse model for studies of HEV71 pathogenesis and for vaccine efficacy and immunogenicity testing, we selected a mouse-adapted variant of HEV71 by serial passage of a recent clinical isolate. We also report on the molecular mechanism of mouse adaptation and virulence of HEV71 in this model.

Methods

Cells and viruses.

African green monkey kidney (Vero) cells (ATCC CCL-81), human rhabdomyosarcoma (RD) cells (ATCC CCL-136), simian virus 40-transformed African green monkey kidney (COS-7) cells (ATCC CRL-1651) and Chinese hamster ovary (CHO) cells (ATCC CCL-61) were maintained in Dulbecco's modified Eagle's medium (DMEM) (MultiCel; Trace Biosciences) supplemented with 5% bovine growth serum (BGS) (MultiSer; Trace Biosciences) and 2 mM L-glutamine. HEV71 strain 26M/AUS/4/99 (HEV71-26M) was isolated in Western Australia in 1999 (McMinn *et al.*, 2001a). HEV71-26M was plaque purified and propagated by six passages in RD cells. To generate mouse-adapted HEV71, parental HEV71-26M was first adapted to growth in CHO cells by six passages at an m.o.i. of 1. CHO-adapted HEV71-26M (CHO-26M) was then passaged six times by i.c. inoculation of

1-day-old BALB/c mice with 10^3 TCID$_{50}$ virus obtained from clarified brain homogenates. Mouse-adapted virus derived from the sixth mouse brain passage was passaged a further two times in Vero cells and designated MP-26M.

RNA extraction, cDNA synthesis and nucleotide sequence analysis.

RNA was extracted from HEV71-infected cell culture supernatants using a QIAamp viral RNA mini kit (Qiagen). First-strand cDNA synthesis was undertaken using SuperScript II reverse transcriptase (Invitrogen); viral cDNA was amplified using PCR SuperMix (Invitrogen) with gene-specific primers and gel purified using a MinElute gel extraction kit (Qiagen). Nucleotide sequences of the whole genome of HEV71-26M, CHO-26M and MP-26M, infectious cDNA clone-derived virus (CDV) genomic fragments and plasmid DNA were determined by automated DNA sequencing using Big Dye Terminator sequencing technology. Sequencing was performed at the Australian Genome Research Facility, University of Queensland, Australia. Sequence analysis was performed using Chromas version 2.3 (Technelysium Pty) and Clone Manager 5/Align Plus 4 software (SciEd Central).

Construction of full-length infectious cDNA clones of HEV71-26M and variants

Full-length infectious cDNA clones of HEV71-26M, CHO-26M and MP-26M were constructed using RT-PCR, restriction enzyme digestion and cloning, as described below. All viral cDNA fragments used for cloning were amplified by PCR using Platinum *Taq* DNA Polymerase High Fidelity (Invitrogen). Competent *Escherichia coli* strain XL10-Gold (Stratagene) was used for cloning and amplification of all plasmid constructs. Clones were screened by restriction enzyme digestion and sequencing. A schematic diagram of the infectious cDNA clones prepared in this study is presented in Fig. 1.

pHEV71-26M.

The full-length cDNA clone of HEV71-26M was constructed in two subgenomic clones, using plasmid pMC18 (Gualano *et al.*, 1998). Plasmid pMC/5′-26M contained nt 1–3114 of HEV71-26M, preceded by a *Sal*I restriction site to facilitate cloning, a T7 RNA polymerase promoter and two additional 5′ G residues to improve transcription efficiency (Boyer & Haenni, 1994). Plasmid pMC/3′-26M contained a *Sal*I restriction site upstream of nt 2809–7409 of HEV71-26M, a 25mer poly(A) tail and unique *Mlu*I and *Not*I restriction sites downstream of the poly(A) tail. pHEV71-26M was then prepared by excising the *Sal*I–*Eco*RI^{2842}fragment from the clone pMC/5′-26M and inserting it into the *Sal*I–*Eco*RI^{2842} site of pMC/3′-26M.
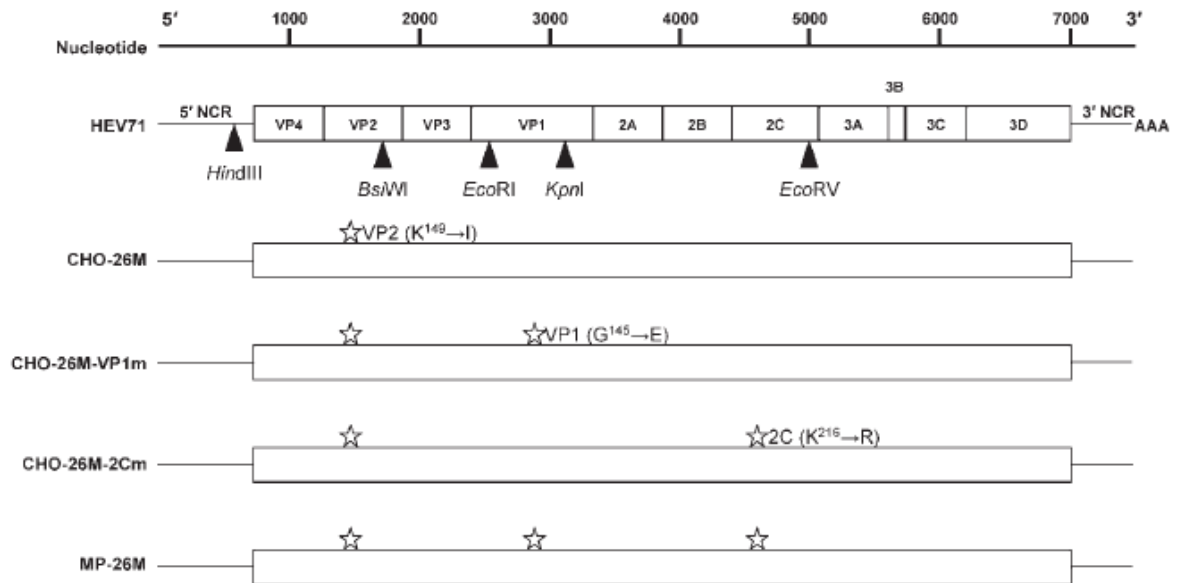
Fig. 1. Schematic representation of the infectious cDNA clones of HEV71-26M, CHO-26M, CHO-26M-VP1m, CHO-26M-2Cm and MP-26M. Genome maps of HEV71-26M and its variants are represented as an open box, with individual genes and non-coding regions (NCRs) indicated for HEV71-26M. Amino acid mutations observed in CHO-26M, CHO-26M-VP1m, CHO-26M-2Cm and MP-26M are shown as open stars. The approximate positions of the restriction enzyme sites used in clone construction are indicated on the HEV71-26M genome.

pCHO-26M.

The full-length cDNA clone of CHO-26M was constructed by PCR amplification of nt 533–3111 of CHO-26M containing the VP2 ($A^{1400}{\rightarrow}T$) mutation. A PCR fragment containing the CHO-26M VP2 ($A^{1400}{\rightarrow}T$) mutation (nt 533–3111) was amplified and digested with *Hin*dIII and *Eco*RI, and then subcloned into similarly digested pBR322 to create pBRCHO. The *Hin*dIII^{968}–*Bsi*WI^{1442} fragment excised from a positive clone (pBRCHO) was then introduced into the corresponding region in pHEV71-26M to create pCHO-26M.

pCHO-26M-VP1m.

An *Eco*RI^{2842}–*Eco*RV^{4819}-digested PCR fragment containing the VP1 ($G^{2876}{\rightarrow}A$) mutation was amplified from MP-26M and subcloned into pBR322 to create pBRMP. The *Eco*RI^{2842}–*Kpn*I^{3062} fragment from pBRMP was then introduced into the corresponding region of pCHO-26M to produce pCHO-26M-VP1m.

pCHO-26M-2Cm.

Both pBRMP and pCHO-26M were digested with *Kpn*I and *Eco*RV to introduce a *Kpn*I^{3062}–*Eco*RV^{4819} fragment from pBRMP into the corresponding region of pCHO-26M to construct

a plasmid containing the MP-26M-associated 2C gene mutation in the CHO-26M background.

pMP-26M.

The EcoRI^{2842}–EcoRV^{4819} fragment was excised from pBRMP and cloned into the corresponding fragment of pCHO-26M to produce a plasmid containing both MP-26M-associated VP1 and 2C mutations in the CHO-26M background.

Transfection and recovery of infectious CDV populations.

Infectious cDNA clones were transfected into COS-7 cells using Lipofectamine 2000 (Invitrogen). Briefly, COS-7 cells were seeded into 12-well tissue-culture trays (CellStar) at a seeding density of 3×10^5 cells per well. After incubation for 18–24 h, cells were washed with PBS (pH 7.4) and replaced with serum-free medium (Optimem; Invitrogen) prior to transfection. The lipid–nucleic acid complex containing 1.6 µg of each full-length cDNA construct, 1.6 µg pCMV-T7Pol expressing the T7 RNA polymerase and 4 µl Lipofectamine 2000 was added to the cells and incubated for 4 h. The transfection medium was then removed and replaced with DMEM supplemented with 2 mM L-glutamine and 2% BGS and the cells incubated for a further 72 h. Transfected cells were subjected to three cycles of freeze–thawing and the supernatants clarified by centrifugation at 1000 g for 15 min. CDV stocks were passaged once on RD cells and stored at −80 °C until required. CDV stocks are designated as such by the prefix CDV to distinguish them from their respective parental virus.

Virus titration and single-step growth kinetics.

TCID$_{50}$ assays were performed on Vero cells and virus titres calculated following the method of Reed & Muench (1938). Vero cell monolayers (10^4 cells per well) in 96-well tissue-culture trays (CellStar) were inoculated with 100 µl 10-fold serial dilutions of each virus stock and incubated for 5 days prior to observation of the presence of cytopathic effect.

RD and CHO cell monolayers grown overnight in 48-well tissue-culture trays (5×10^4 cells per well) were infected at an m.o.i. of 5 for 1 h at 37 °C. Inoculated cells were then washed three times with PBS and overlaid with 200 µl maintenance medium (DMEM supplemented with 2 mM L-glutamine and 2% BGS) per well. Cells and supernatants were collected every 4 h for 24 h, with the first time point (time 0) collected immediately after the addition of the maintenance medium. Samples at each time point were frozen and thawed three times and clarified by centrifugation at 8000 g for 10 min prior to the determination of the virus titre by the TCID$_{50}$ assay.

Mouse virulence assays.

Specific-pathogen-free pregnant BALB/c mice were obtained from the Animal Resources Centre, Perth, Australia. All experiments were performed on the ensuing litters of newborn mice. Mice were housed in filter-topped cages on a deep litter of sawdust and were provided

with food and water *ad libitum*. All mouse studies were approved by the institutional Animal Experimentation Ethics Committee.

In order to minimize distress, 50% humane end points (HD_{50}) were used instead of 50% lethal end points; HD_{50} values are calculated from the time of onset of lethal infection (see below) instead of waiting until death ensues. Humane end-point assays have been found to be almost identical to lethal end-point virulence assays (Wright & Phillpotts, 1998).

Groups of four to ten 1- or 7-day-old BALB/c mice were infected with serial 10-fold dilutions of virus by i.c., i.p. or i.m. inoculation and HD_{50} values were calculated by the method of Reed & Muench (1938). Mean survival time was calculated in groups of ten 7-day-old BALB/c mice after i.m. inoculation of $10^4 TCID_{50}$ virus. Infected mice were observed twice daily for clinical signs of illness up to 21 days post-infection (p.i.). Mice that developed clinical signs of HEV71 infection, including dehydration, lack of feeding, a hunched back, paresis and fore- and/or hindlimb paralysis, were sacrificed by an overdose of pentobarbitone sodium ($100\,mg\,kg^{-1}$ by i.p. injection).

Tissue distribution and histological studies.

Groups of 15 7-day-old BALB/c mice were infected by the i.m. route with $10^4 TCID_{50}$ virus. At the indicated times p.i., three mice from each group were anaesthetized by i.p. injection with a mixture of xylazine ($20\,mg\,ml^{-1}$) and ketamine ($100\,mg\,ml^{-1}$) in PBS at 5 μl (g body weight)$^{-1}$. Whole blood was collected by intracardiac puncture and stored at −80 °C. After perfusion with PBS, tissue samples were then collected, weighed individually, snap-frozen in liquid nitrogen and stored at −80 °C. Tissues were homogenized with a Dounce homogenizer and the homogenates prepared as 10% (w/v) suspensions in Hanks' balanced salt solution (pH 8.0). Virus titres in each tissue homogenate were determined by $TCID_{50}$ assay; titres are expressed as $TCID_{50}$ (ml whole blood)$^{-1}$or (g tissue)$^{-1}$ ($TCID_{50}\,ml^{-1}$ or g^{-1}).

Tissues for histological analysis were snap-frozen in Tissue-Tek OCT compound (Sakura Finetek USA) in liquid nitrogen. Frozen tissue sections (6 μm) were cut on a microtome and then mounted onto Superfrost glass slides (VWR Labware), fixed in 10% formalin (pH 8.0) and stained with haematoxylin and eosin.

Results

Mouse-adapted HEV71 has increased virulence in newborn mice

Infection of newborn mice by i.c. inoculation of HEV71-26M does not cause clinically overt disease. In order to create a mouse-adapted strain, HEV71-26M was passaged six times (m.o.i. of 1) in CHO cells to produce a CHO cell-adapted virus strain (CHO-26M). CHO-26M was then passaged six times by i.c. inoculation of newborn BALB/c mice ($10^3 TCID_{50}$ virus in 10% mouse brain suspensions). By the fourth mouse passage, infection caused 100% mortality (data not shown). Virus at the sixth mouse passage was cultured twice on Vero cells to generate virus stocks and was designated MP-26M. As both HEV71-26M
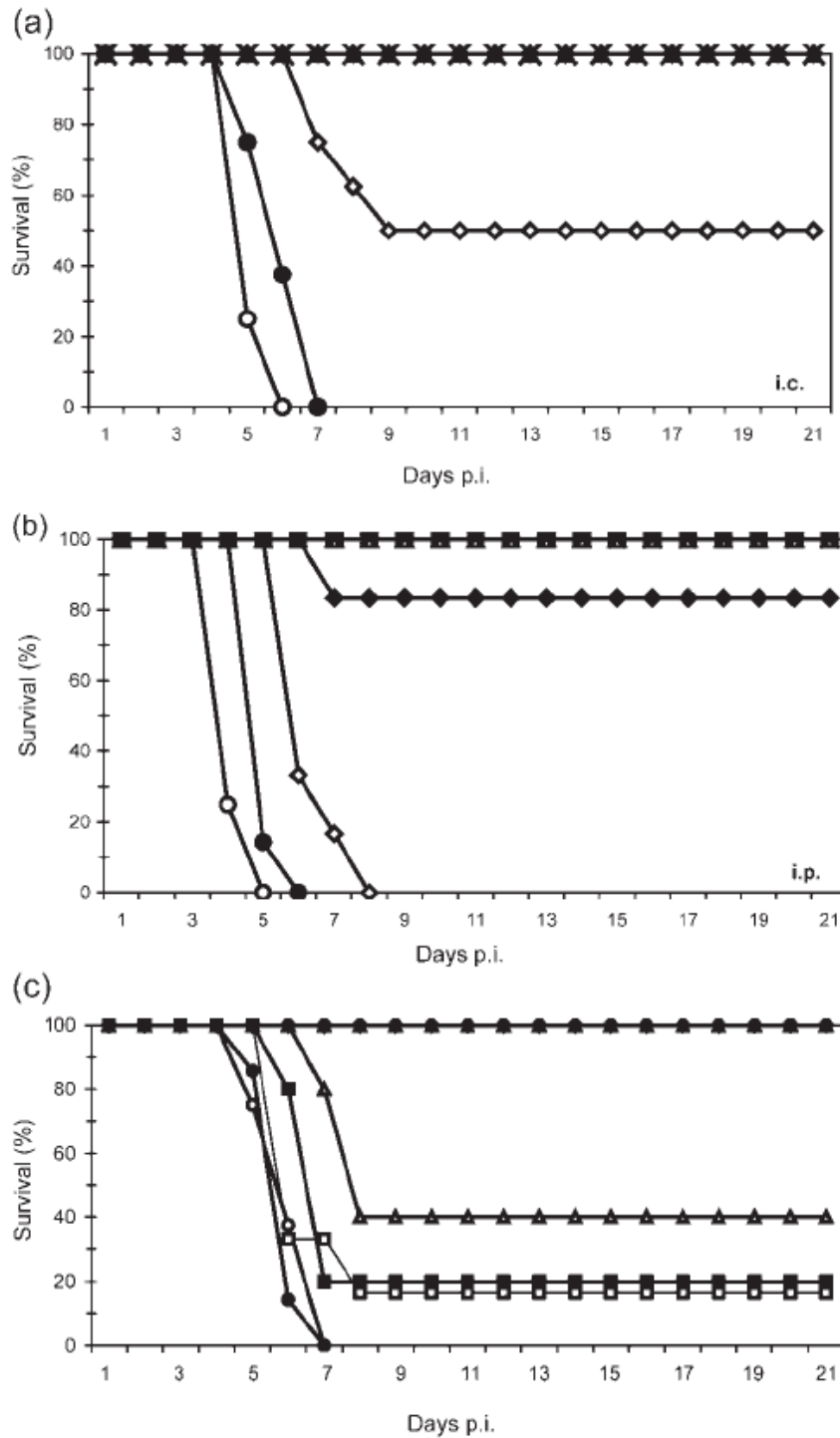
Fig. 2. Mortality and age-related susceptibility of BALB/c mice infected with HEV71-26M, CHO-26M or MP-26M. One-day-old BALB/c mice were inoculated by the i.c. (a) or i.p. (b) route with 10-fold serial dilutions of HEV71-26M, CHO-26M or MP-26M. ○, 10^1 TCID$_{50}$MP-26M; •, 10^0 TCID$_{50}$ MP-26M; ◊, 10^{-1} TCID$_{50}$ MP-26M; □, 10^{-2} TCID$_{50}$ MP-26M; □, 10^{-3} TCID$_{50}$ MP-26M; ×, 10^1TCID$_{50}$ CHO-26M; ▵, 10^1TCID$_{50}$ HEV71-26M. (c) BALB/c mice were inoculated by the i.c. route with 10 HD$_{50}$ MP-26M at the following ages, observed for 21 days and the percentage survival calculated. ○, 1 day old; •, 3 days old; □, 5 days old; ▪, 7 days old; ▵, 9 days old; ▲, 14 days old; ◊, 21 days old.

and CHO-26M are non-virulent in newborn BALB/c mice (Fig. 2), CHO-26M was selected as the parental strain for comparison with MP-26M in mouse virulence assays.

In order to compare the virulence of MP-26M and CHO-26M, groups of five to ten 1-day-old BALB/c mice were inoculated with 10-fold serial dilutions (10^1–10^{-3} TCID$_{50}$) of CHO-26M or MP-26M by i.c. or i.p. inoculation. MP-26M showed significantly greater virulence in newborn BALB/c mice than CHO-26M (Fig. 2). Mice infected with CHO-26M did not develop clinical signs of infection at any virus dose. By contrast, all MP-26M-infected mice developed fore- and/or hindlimb paralysis, irrespective of the route of inoculation (data not shown). Mice succumbed to MP-26M infection between 4 and 9 days after i.c. inoculation (Fig. 2a) and between 3 and 8 days after i.p. inoculation (Fig. 2b). HD$_{50}$ values for MP-26M were 5.0×10^{-1} TCID$_{50}$ and 3.2×10^{-1} TCID$_{50}$ after i.c. and i.p. inoculation, respectively. By contrast, both HEV71-26M and CHO-26M had HD$_{50}$ values greater than 10^6 TCID$_{50}$ (data not shown).

Susceptibility of BALB/c mice to infection with mouse-adapted HEV71

The age dependence of BALB/c mice to infection with MP-26M after i.c. inoculation was investigated by infecting groups of four to eight mice at 1, 3, 5, 7, 9, 14 and 21 days of age with 10 HD$_{50}$ (3.2 TCID$_{50}$) of MP-26M; the results are shown in Fig. 2(c). Mice aged between 1 and 3 days had a similar mortality profile, with death commencing at 4 days p.i. and reaching 100% mortality by 7 days p.i. Mice aged 5–7 days at infection survived until day 5 p.i. and reached mortalities of 83.5 and 80.0%, respectively, by 8 days p.i. All 9-day-old mice survived to 6 days p.i. and 60.0% mortality was observed in this age group at 8 days p.i. Mice infected with MP-26M at 14 days of age and older did not develop clinical signs of infection and all survived to 21 days p.i. Seven-day-old mice were selected for all subsequent experiments.

In order to determine whether host susceptibility to MP-26M was dependent on virus dose and route of inoculation, groups of four to eight 7-day-old mice were inoculated with 10-fold serial dilutions of virus by either the i.c., i.p. or i.m. route; the results are shown in Table 1. HD$_{50}$ values of 5×10^2, 3.4×10^3 and 1.5×10^2 TCID$_{50}$ were calculated after i.c., i.p. and i.m. inoculation, respectively. A mortality rate of 100% was observed at virus doses greater than 3.4×10^4 TCID$_{50}$ for all three routes of inoculation. At a dose of 3.4×10^3 TCID$_{50}$, 100% mortality was observed after i.m. inoculation, but only 50.0 and 85.7% mortality was observed after i.p. and i.c. inoculation, respectively. Mortality rates after i.c. and i.m. inoculation of 3.4×10^2 TCID$_{50}$ MP-26M were 42.9 and 25.0%, respectively; all i.p.-inoculated mice survived infection with this virus dose. These data indicated that MP-26M induces a fatal disease in BALB/c mice in an age-, dose- and route-of-inoculation-dependent manner. All MP-26M-infected mice showed similar clinical signs of infection, irrespective of the route and dose of inoculation.

Table 1. Percentage mortality in 7-day-old BALB/c mice after MP-26M infection

Groups of four to eight mice were inoculated with 10-fold serial dilutions of MP-26M by the i.c. (10 µl), i.p. (50 µl) or i.m. (5 µl) route and infected mice were observed twice daily for clinical signs of illness up to 14 days p.i.

Route of inoculation	Mortality (%) at the indicated virus dose ($TCID_{50}$)						HD_{50} ($TCID_{50}$)*
	3.4×10^0	3.4×10^1	3.4×10^2	3.4×10^3	3.4×10^4	3.4×10^5	
i.c.	0	0	42.9	85.7	100	100	5.0×10^2
i.p.	0	0	0	50	100	100	3.4×10^3
i.m.	0	0	25	100	100	100	1.5×10^2

*HD_{50} values were determined using the method of Reed & Muench (1938).

Tissue distribution of CHO-26M and MP-26M in 7-day-old BALB/c mice after i.m. inoculation

In order to investigate differences in tissue tropism between MP-26M and CHO-26M, the distribution of both viruses in host tissues was compared after i.m. inoculation. Groups of 7-day-old BALB/c mice (15 per group) were inoculated by the i.m. route with 1.5×10^4 $TCID_{50}$ MP-26M or CHO-26M. Whole blood and tissue samples, including heart, liver, spleen, skeletal muscle and brain, were collected at 1, 3, 5 and 7 days p.i. and virus titres determined by $TCID_{50}$ assay (Fig. 3).

CHO-26M was isolated from the site of inoculation at all times p.i., with the virus titre peaking at >10^6 $TCID_{50}$ g^{-1} at 3 days p.i. (Fig. 3a). CHO-26M was also detected at a single uninoculated skeletal muscle site of three individual mice at 1, 3 and 5 days p.i. and in the brains of two individual mice at 5 and 7 days p.i. (data not shown), indicating that CHO-26M is capable of viraemic spread in a proportion of hosts. Despite this, clinically apparent disease was not observed in any CHO-26M-infected mice at any time p.i.

For MP-26M-infected mice, virus was first detected on day 1 in the inoculated left hindlimb (mean titre 8.9×10^4 $TCID_{50}$ g^{-1}); the virus titre peaked in the left hindlimb at day 3 (mean titre 2.8×10^6 $TCID_{50}$ g^{-1}) and remained high (>$10^6 TCID_{50}$ g^{-1}) at 5 and 7 days p.i. (Fig. 3b). Viraemia was first detected at 3 days p.i. and was maintained at similar titres (~10^3 $TCID_{50}$ ml^{-1}) throughout the experiment. Virus first appeared in heart and spleen and in skeletal muscle of the uninoculated limbs at 3 days p.i. and coincided with viraemia, suggesting haematogenous spread (Fig. 3b). All MP-26M-infected mice developed flaccid limb paralysis by 5 days p.i. Mice that survived to day 7 also developed a hunched posture, listlessness and weight loss. Virus titres in uninoculated and inoculated skeletal muscle groups were almost identical at 5 and 7 days p.i., indicating that skeletal muscle is the primary site of MP-26M replication and the likely source of viraemia. Virus appeared in the central nervous system of all MP-26M-infected mice at 5 days p.i., 48 h after the onset of viraemia (Fig. 3b).
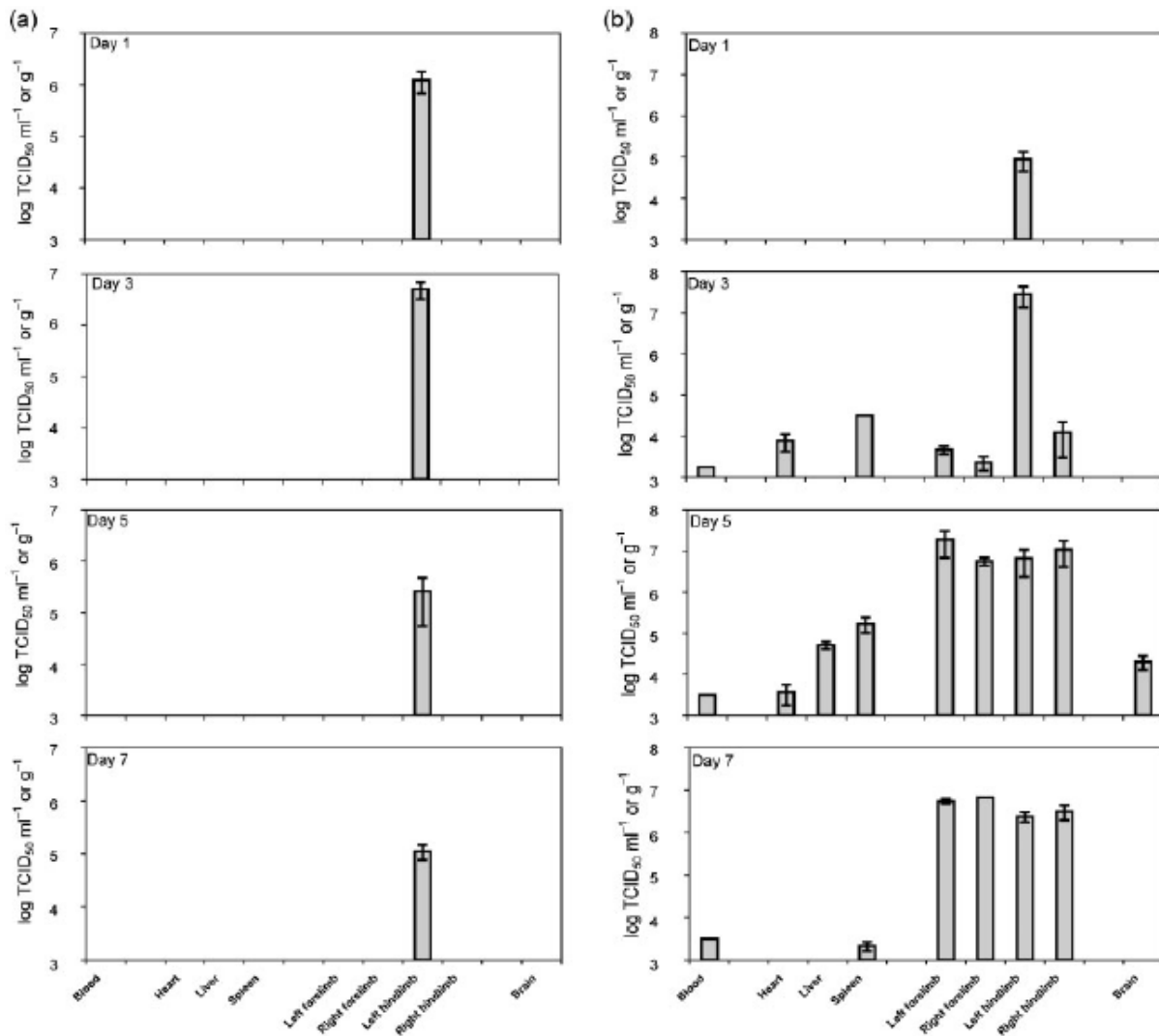
Fig. 3. Growth of CHO-26M and MP-26M in 7-day-old BALB/c mice. Seven-day-old mice were inoculated by the i.m. route with 1.5×10^4 $TCID_{50}$CHO-26M (a) or MP-26M (b). Whole blood and the indicated tissues were prepared as 10% suspensions in Hanks' balanced salt solution (pH 8.0) at the indicated times p.i. and titrated by $TCID_{50}$ assay. Each time point represents the mean tissue titre in at least two mice ($TCID_{50}ml^{-1}$ or g^{-1}).

Histological analysis of HEV71-infected tissues

In order to characterize further the pathogenesis of MP-26M and CHO-26M in 7-day-old mice, histological changes in the tissues of virus-infected mice were examined. The most notable histological changes in CHO-26M-infected mice were identified in skeletal muscle. Neutrophil infiltration was observed in the left (inoculated) hindlimb and in the right forelimb at 5 and 7 days p.i. (Fig. 4). Mild neutrophil infiltration was also observed in skeletal muscle of both right fore- and hindlimbs at 7 days p.i. No obvious abnormalities were observed in the heart, liver or spleen of CHO-26M-infected mice at any time p.i. However, solitary lymphocytic inflammatory foci were observed in the cervical and lumbar spinal cord sections of two CHO-26M-infected mice at 7 days p.i. (Fig. 4). By contrast, intense neutrophil infiltration and necrosis of skeletal muscle was observed at the site of inoculation in MP-26M-infected mice at 3 days p.i. By 5 days p.i., marked neutrophil infiltration was observed in all skeletal muscle groups, with necrotizing myositis developing by 7 days p.i. (Fig. 4). In

addition, mild neutrophil infiltration was observed in single thoracic and lumbar spinal cord sections of two mice at 7 days p.i. (Fig. 4). No obvious histological abnormality was observed in heart, liver or spleen tissue at any time after infection, despite the growth of MP-26M in these tissues (Fig. 3b).
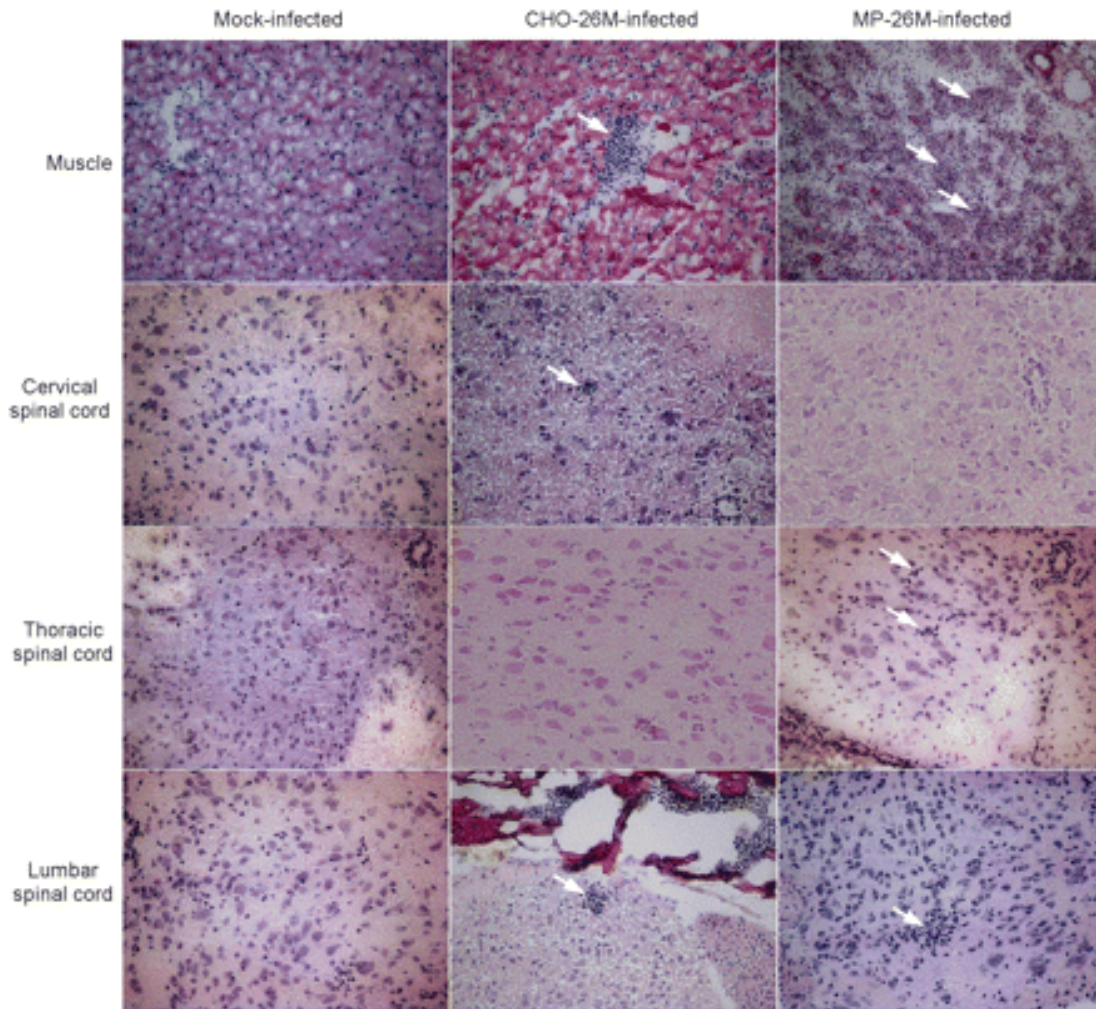

Fig. 4. Histological features of skeletal muscle and spinal cord in 7-day-old BALB/c mice infected by the i.m. route with HEV71. Seven-day-old BALB/c mice were infected by the i.m. route with 10^4 TCID$_{50}$ CHO-26M or MP-26M. Three mice were sacrificed on days 1, 3, 5 and 7 p.i. and tissues collected as outlined in Methods. In MP-26M-infected tissues (right column), neutrophil infiltration and necrosis of skeletal muscle (arrows) were seen at 7 days p.i., and infiltrating neutrophils (arrows) were also observed in thoracic and lumbar spinal cord sections of two mice at 7 days p.i. In CHO-26M-infected tissues (middle column), neutrophil infiltration (arrow) was seen in skeletal muscle and in cervical and lumbar spinal cord sections (arrows) of two mice at 7 days p.i. Mock-infected tissues are shown in the left column. Magnification, ×200.

Nucleotide sequence comparison of the genomes of HEV71-26M, CHO-26M and MP-26M

The complete nucleotide and deduced amino acid sequences of HEV71-26M, CHO-26M and MP-26M were compared in order to identify mutations associated with adaptation of virus to growth in CHO cells and in BALB/c mice (Fig. 5c⇓). Comparison of the HEV71-26M and CHO-26M sequences revealed four nucleotide differences, all of which were located in the virus polyprotein open reading frame (ORF); only one of these mutations resulted in a change in the deduced amino acid sequence, in VP2 ($K^{149} \rightarrow I$). Four additional nucleotide sequence changes were identified in the ORF of MP-26M, and two of these mutations resulted in deduced amino acid changes in VP1 ($G^{145} \rightarrow E$) and 2C ($K^{216} \rightarrow R$). No nucleotide sequence changes were observed in the 5′ and 3′ non-coding regions of all three virus populations. Furthermore, the two mutations identified in the 2C gene were not located within the HEV71 *cis*-replication element (data not shown).
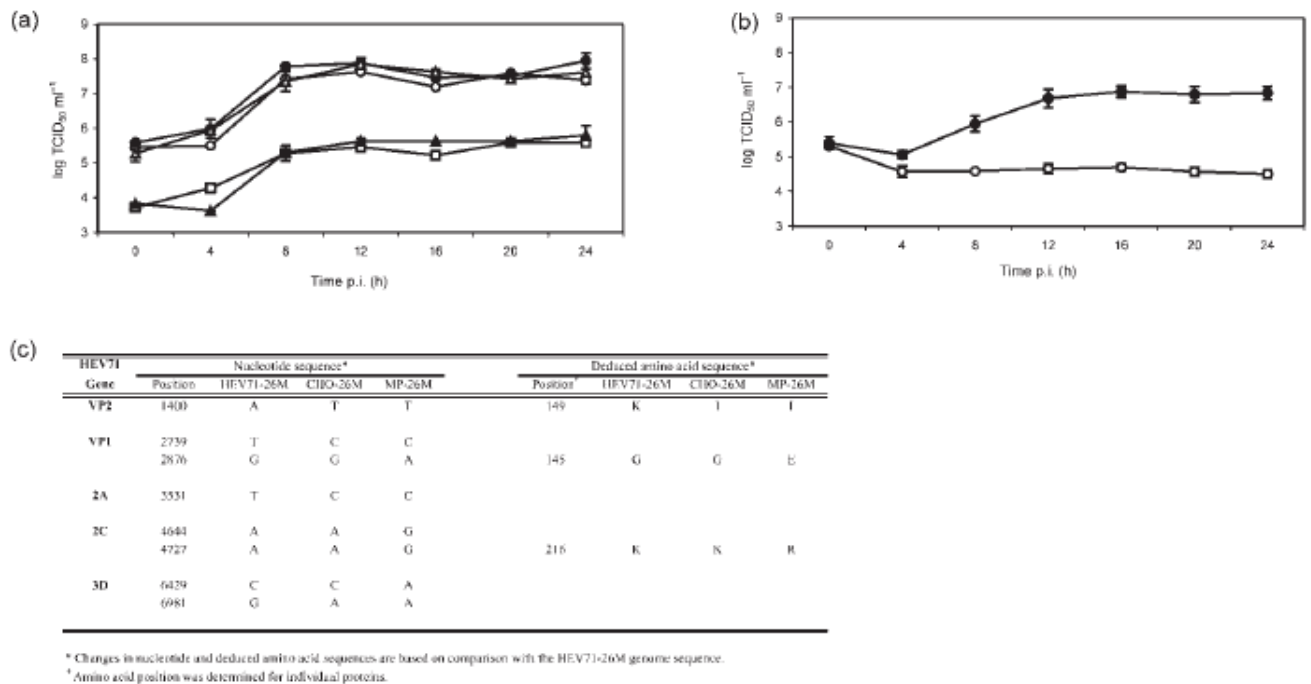

(c)

HEV71 Gene	Nucleotide sequence*				Deduced amino acid sequence*			
	Position	HEV71-26M	CHO-26M	MP-26M	Position†	HEV71-26M	CHO-26M	MP-26M
VP2	1400	A	T	T	149	K	I	I
VP1	2739	T	C	C				
	2876	G	G	A	145	G	G	E
2A	3531	T	C	C				
2C	4644	A	A	G				
	4727	A	A	G	216	K	K	R
3D	6429	C	C	A				
	6981	G	A	A				

* Changes in nucleotide and deduced amino acid sequences are based on comparison with the HEV71-26M genome sequence.
† Amino acid position was determined for individual proteins.

Fig. 5. Growth in cell culture and mutations identified in CDV HEV71-26M and variants. RD and CHO cells were inoculated with the indicated virus (m.o.i. of 5 $TCID_{50}$ per cell) as described in Methods. Tissue-culture supernatants were collected at the indicated times and virus titres determined by $TCID_{50}$ assay; all assays were performed in triplicate. Inoculated virus was back-titrated to ensure an m.o.i of 5 $TCID_{50}$ per cell in each experiment. (a) RD cells were inoculated with CDV-HEV71-26M (○), CDV-CHO-26M (•), CDV-CHO-26M-VP1m (▲), CDV-CHO-26M-2Cm (△) or CDV-MP-26M (□). (b) CHO cells were inoculated with CDV-HEV71-26M (○) or CDV-CHO-26M (•). (c) Nucleotide and amino acid changes identified in the genomes of HEV71-26M, CHO-26M and MP-26M.

A single amino acid substitution in VP2 ($K^{149} \rightarrow I$) increases the growth of HEV71 in CHO cells

In order to determine whether the VP2 ($K^{149} \rightarrow I$) mutation was responsible for the improved growth of virus in cell culture, single-step growth analysis was undertaken in RD and CHO cells using CDV populations of HEV71-26M (CDV-HEV71-26M) and CHO-26M (CDV-CHO-26M). The single-step growth kinetics and virus yields of both viruses were almost identical in RD cells (Fig. 5a). By contrast, CDV-CHO-26M replicated more efficiently than CDV-HEV71-26M in CHO cells, with maximum titres more than 100-fold higher than that of parental virus (Fig. 5b).

A single amino acid substitution in VP1 ($G^{145} \rightarrow E$) determines the mouse virulence phenotype of HEV71

In order to identify genetic changes associated with the increased virulence observed in mouse-adapted virus (MP-26M), 7-day-old BALB/c mice (eight to 12 per group) were inoculated by the i.m. route with 10^4 $TCID_{50}$ of each infectious CDV population (Table 2). As expected, the CDV-HEV71-26M and CDV-CHO-26M virus populations caused no observable morbidity or mortality in infected mice. By contrast, CDV-MP-26M caused 100 % mortality with a mean (±SEM) survival time of 5.0 (±0.0) days p.i. Interestingly, CDV-CHO-26M-VP1m and CDV-CHO-26M-2Cm had markedly different mouse virulence phenotypes. CDV-CHO-26M-2Cm caused no observable signs of infection and no mortality in 7-day-old mice. By contrast, CDV-CHO-26M-VP1m caused 100 % morbidity and mortality, with a mean survival time of 4.9 (±0.35) days p.i., similar to the parental MP-26M.

Table 2.

Percentage mortality and mean survival of 7-day-old BALB/c mice infected by the i.m. route with CDV HEV71 variants

Virus*	Mortality (%)†	Mean survival time (days ± SEM)†	HD_{50} ($TCID_{50}$)‡
CDV-HEV71-26M	0	>14	>10^4
CDV-CHO-26M	0	>14	>10^4
CDV-CHO-26M-2Cm	0	>14	>10^4
CDV-CHO-26M-VP1 m	100	4.9 ± 0.35	1.6
CDV-MP-26M	100	5.0 ± 0.0	5

*CDV populations were passaged once in RD cells prior to use in these experiments.

†Groups of 7-day-old mice (eight to 12 per group) were inoculated by the i.m. route (5 µl) with 10^4 $TCID_{50}$ of each CDV population and observed twice daily for clinical signs of illness up to 14 days p.i.; mean survival time (±SEM) is expressed as number of days.

‡Groups of 7-day-old mice (eight to ten per group) were inoculated by the i.m. route (5 µl) with 10-fold serial dilutions (10^0–10^{-4} $TCID_{50}$) of each CDV population and observed twice daily for clinical signs of illness up to 14 days p.i.; HD_{50} values were determined using the method of Reed & Muench (1938).

HD_{50} values for all CDV HEV71 variants were determined by i.m. inoculation of 7-day-old BALB/c mice (eight to ten per group) with serial 10-fold dilutions of virus. Only CDV-MP-26M and CDV-CHO-26M-VP1m produced measurable HD_{50} values of 5.0 and 1.6 $TCID_{50}$, respectively (Table 2). This result clearly demonstrated that a non-conservative amino acid substitution in VP1 ($G^{145}{\rightarrow}E$) alone was sufficient to confer the mouse virulence phenotype observed in both wild-type and clone-derived MP-26M.

The growth of each of the infectious CDV populations was examined in RD cells. CDV-HEV71-26M, CDV-CHO-26M and CDV-CHO-26M-2Cm displayed identical single-step growth kinetics in RD cells, reaching maximum titres of approximately $10^{7.5}$ $TCID_{50}$ ml^{-1} at 12 h p.i. (Fig. 5a). The two virus strains containing the VP1 ($G^{145}{\rightarrow}E$) mutation, CDV-CHO-26M-VP1m and CDV-MP-26M, grew poorly in RD cells compared with the other viruses, with peak titres approximately 100-fold lower than CDV-HEV71-26M, CDV-CHO-26M and CDV-CHO-26M-2Cm at 12 h p.i. (Fig. 5a).

Stability of the MP-26M-associated VP1 ($G^{2876}{\rightarrow}A$) and 2C ($A^{4727}{\rightarrow}G$) mutations during passage in 7-day-old BALB/c mice and in RD cell culture

Amino acid substitutions introduced during mouse adaptation may revert to that of the parental virus during cell-culture passage (Jia *et al.*, 2001). To determine whether the amino acid substitutions observed in VP1 and/or 2C of mouse-adapted virus would revert to the wild-type sequence during passage in cell culture, the stability of these mutations was determined by examining the VP1 ($G^{2876}{\rightarrow}A$) and 2C ($A^{4727}{\rightarrow}G$) nucleotide sequences of CDV-MP-26M at increasing passage levels in RD cells. CDV-MP-26M was cultured at an m.o.i. of 1 for five passages in RD cells and viral RNA was extracted from culture supernatants at approximately 16–18 h p.i. at each passage level. The VP1 and 2C genes were amplified by RT-PCR and their nucleotide sequences determined (Table 3). The 2C gene mutation was retained during the five passages in RD cells. By contrast, the VP1 gene mutation had reverted to the wild-type EV71-26M sequence by the second RD cell passage.

As the VP1 ($G^{2876}{\rightarrow}A$) mutation rapidly reverted to the wild-type sequence during passage in RD cells, the stability of the mouse-adapted VP1 and 2C mutations was also investigated during passage in mice. CDV-MP-26M was passaged five times in 7-day-old BALB/c mice by i.m. inoculation (10^{4} $TCID_{50}$). Viral genomic RNA recovered from brain and muscle specimens at each passage level was amplified by RT-PCR using primers specific for the VP1 and 2C genes and the amplicons were sequenced (Table 3). In contrast to RD cell passage, both the VP1 ($G^{2876}{\rightarrow}A$) and 2C ($A^{4727}{\rightarrow}G$) mutations persisted for five passages in BALB/c mice.

Discussion

Similar to all human enteroviruses, HEV71 has a limited host range, with humans the only known natural host. Although Old World monkeys such as cynomolgus, rhesus and African green monkeys can be infected experimentally with HEV71 (Chumakov *et al.*, 1979; Hashimoto & Hagiwara, 1982; Hashimoto *et al.*, 1978), other animal species, including rodents, are resistant to infection. In a previous study (Chen *et al.*, 2004) as well as in our

Table 3. Stability of the MP-26M-associated VP1 ($G^{2876} \rightarrow A$) and 2C ($A^{4727} \rightarrow G$) nucleotide mutations during passage in RD cells and in 7-day-old BALB/c mice

CDV populations were used in these experiments.

Passage no.	RD cells*		BALB/c mouse brain†		BALB/c mouse skeletal muscle†	
	VP1	2C	VP1	2C	VP1	2C
1	A	G	A	G	A	G
2	G	G	A	G	A	G
3	G	G	A	G	A	G
4	G	G	A	G	A	G
5	G	G	A	G	A	G

*RD cells were infected with CDV MP-26M at an m.o.i. of 1 for five serial passages. RNA was extracted from infected cell-culture supernatants at 18 h p.i., the VP1 and 2C genes were amplified by RT-PCR and the amplicons were sequenced.

†Groups of 7-day-old BALB/c mice were infected by the i.m. route (10^4 TCID$_{50}$) with CDV MP-26M for five serial passages. RNA was extracted from brain and skeletal muscle tissue collected at 5 days p.i., the VP1 and 2C genes were amplified by RT-PCR and the amplicons were sequenced.

study, a mouse-adapted strain of HEV71 was selected by serial passage of virus in mouse brain. However, the molecular mechanism of host-range adaptation by HEV71 has not been clarified.

In order to select a mouse-adapted strain of HEV71, the virus was firstly passaged six times in CHO cells. A non-conservative amino acid substitution in the capsid protein VP2 ($K^{149} \rightarrow I$) was identified in CHO-adapted virus. Comparison of the single-step growth kinetics of CDV-HEV71-26M and CDV-CHO-26M in CHO cells clearly demonstrated that the VP2 ($K^{149} \rightarrow I$) mutation was responsible for the improved growth of CDV-CHO-26M in this cell line. Chen *et al.* (2004) adapted a clinical isolate of HEV71 (MP-4643) to grow in random-bred ICR mice. Mice infected by the i.p. route with the mouse-adapted strain died in an age- and virus dose-dependent manner. Interestingly, the only capsid protein mutation identified in the mouse-adapted virus selected by Chen *et al.* (2004) was located at the same position in VP2, with the positively charged lysine residue substituted by a non-polar leucine residue (Wang *et al.*, 2004). Thus, repeated selection at this site in VP2 during mouse (Chen *et al.*, 2004) or CHO cell (our study) passage suggests that this residue plays an important role in the infection cycle of HEV71 in rodent cells.

The VP2 mutation identified in CHO-26M is located in the EF loop, a major neutralizing antigenic site for the related poliovirus (Burke *et al.*, 1991). VP2 forms part of a deep cleft on the virion surface of poliovirus that functions as the site of virion attachment to the cellular receptor (Hogle *et al.*, 1985). In the related poliovirus, amino acid residues in the EF loop and on the inner surface of the N terminus of VP2 have been associated with mouse adaptation (Couderc *et al.*, 1994, 1993, 1996). However, the VP2 ($K^{149} \rightarrow I$) mutation identified in CHO-26M was not sufficient to confer the mouse virulent phenotype, but only conferred improved

growth in CHO cells. Studies of virus binding and internalization in CHO cells will help to clarify the mechanism by which this mutation confers CHO cell adaptation.

In our study, only viruses expressing the VP1 ($G^{145}\rightarrow E$) mutation (MP-26M and CHO-26M-VP1m) were virulent in 7-day-old BALB/c mice, indicating that the VP1 ($G^{145}\rightarrow E$) change is a major genetic determinant of mouse adaptation and virulence. Arita *et al.* (2008) recently demonstrated an identical mutation responsible for adaptation of HEV71 to growth in SCID/NOD mice. This amino acid substitution was located on the surface-exposed DE loop of VP1. Amino acid mutations in the DE loop of the poliovirus VP1 protein display altered heat-induced and receptor-mediated capsid conformational changes (Colston & Racaniello, 1995; Martin *et al.*, 1988, 1991; Wien *et al.*, 1997). Taken together, these data suggest that mouse adaptation by HEV71 may involve an early step in virus replication, in particular a change in the specificity of receptor binding. It is likely that parental HEV71-26M is unable to infect mice due to an inability to bind to or enter mouse cells in order to initiate infection. Alternatively, the VP1 $G^{145}\rightarrow E$ mutation may allow HEV71 to undergo mouse cell-specific post-binding capsid conformational changes or cell penetration. Further investigation is needed to understand the mechanism by which this mutation confers mouse adaptation.

Residue 145 of HEV71 VP1 is highly variable and several residues, including glycine, glutamic acid, arginine and alanine, have been identified in field isolates (Cardosa *et al.*, 2003; McMinn *et al.*, 2001b). Moreover, we could not isolate a CDV population that included only the $G^{145}\rightarrow E$ mutation due to reversion to the wild-type sequence after a single passage in RD cells. This suggests that the CHO-associated VP2 residue I^{149} may help to stabilize VP1 residue E^{145} via an as-yet-unknown interaction between these two capsid proteins. Furthermore, the VP2 and VP1 interaction may cooperate to introduce structural change in the virion that either allows the recognition of a mouse cell receptor or may facilitate receptor-mediated conformational changes after attachment.

In addition to the VP1 ($G^{145}\rightarrow E$) mutation identified in MP-26M, a second amino acid substitution was identified in protein 2C ($K^{216}\rightarrow R$). This mutation was in a different location to the four amino acid substitutions identified in the protein 2C of the mouse-adapted strain MP-4643 (Chen *et al.*, 2004). Protein 2C functions as a nucleotide triphosphatase and as a director of viral replication complexes to cell membranes (Pfister & Wimmer, 1999; Teterina *et al.*, 2001), and may also play a role in virion assembly (Li & Baltimore, 1990; Vance *et al.*, 1997). In our study, the 2C ($K^{216}\rightarrow R$) mutation was not responsible for the mouse virulence phenotype. Furthermore, no differences in either cell-culture growth characteristics or plaque morphology were identified between viruses expressing the wild-type (lysine) or mutant (arginine) residue at position 216 in 2C (data not shown). Thus, the significance of the protein 2C mutation in mouse adaptation remains unclear.

We have shown that skeletal muscle is the primary site of HEV71 replication in mice. As expected, mouse-adapted virus grew more efficiently in skeletal muscle than parental virus, yielding approximately 10-fold higher titres. Histological analysis of skeletal muscle showed that infection with CHO-26M induced only mild neutrophil infiltration, whereas infection with mouse-adapted virus induced marked neutrophil infiltration and severe necrotizing

myositis. The presence of necrotizing myositis in MP-26M-infected mice and a lack of evidence of central nervous system disease suggests that the flaccid paralysis observed was due primarily to myositis.

In conclusion, we characterized the molecular basis of CHO cell and mouse adaptation by HEV71. An amino acid change in VP2 ($K^{149}{\rightarrow}I$) was solely responsible for adaptation of virus to growth in CHO cells. Moreover, an amino acid change in VP1 ($G^{145}{\rightarrow}E$) was solely responsible for mouse adaptation and increased virulence in BALB/c mice. The CHO cell and mouse adaptation determinants are likely to be involved in an early event in virus replication, such as virus binding and penetration of the cell surface. The identification of viral genomic regions responsible for the expanded host range and increased virulence in mice has significantly enhanced our understanding of the molecular biology of HEV71. Furthermore, knowledge gained from this study will assist in furthering research on virulence of this increasingly important human pathogen.

Acknowledgements

References

Arita, M., Shimizu, H., Nagata, N., Ami, Y., Suzaki, Y., Sata, T., Iwasaki, T. & Miyamura, T. (2005). Temperature-sensitive mutants of enterovirus 71 show attenuation in cynomolgus monkeys. *J Gen Virol* **86**, 1391–1401.

Arita, M., Ami, Y., Wakita, T. & Shimizu, H. (2008). Cooperative effect of the attenuation determinants derived from poliovirus Sabin 1 strain is essential for attenuation of enterovirus 71 in the NOD/SCID mouse infection model. *J Virol* **82**, 1787–1797.

Boyer, J. C. & Haenni, A. L. (1994). Infectious transcripts and cDNA clones of RNA viruses. *Virology* **198**, 415–426.

Burke, K. L., Almond, J. W. & Evans, D. J. (1991). Antigen chimeras of poliovirus. *Prog Med Virol* **38**, 56–68.

Cardosa, M. J., Perera, D., Brown, B. A., Cheon, D. S., Chan, H. M., Chan, K. P. & McMinn, P. C. (2003). Molecular epidemiology of enterovirus 71 strains associated with recent outbreaks in the Asia–Pacific region: comparative analysis based on the VP1 and VP4 genes. *Emerg Infect Dis* **9**, 461–468.

Chen, Y. C., Yu, C. K., Wang, Y. F., Liu, C. C., Su, I. J. & Lei, H. Y.(2004). A murine oral enterovirus 71 infection model with central nervous system involvement. *J Gen Virol* **85**, 69–77.

Chumakov, M., Voroshilova, M., Shindarov, L., Lavrova, I., Gracheva, L., Koroleva, G., Vasilenko, S., Brodvarova, I., Nikolova, M. & other authors (1979). Enterovirus 71 isolated from cases of epidemic poliomyelitis-like disease in Bulgaria. *Arch Virol* **60**, 329–340.

Colston, E. M. & Racaniello, V. R. (1995). Poliovirus variants selected on mutant receptor-expressing cells identify capsid residues that expand receptor recognition. *J Virol* **69**, 4823–4829.

Couderc, T., Hogle, J., Le Blay, H., Horaud, F. & Blondel, B. (1993). Molecular characterization of mouse-virulent poliovirus type 1 Mahoney mutants: involvement of residues of polypeptides VP1 and VP2 located on the inner surface of the capsid protein shell. *J Virol* **67**, 3808–3817.

Couderc, T., Guedo, N., Calvez, V., Pelletier, I., Hogle, J., Colbere-Garapin, F. & Blondel, B. (1994). Substitutions in the capsid of poliovirus mutants selected in human neuroblastoma cells confer on the Mahoney type 1 strain a phenotype neurovirulent in mice. *J Virol* **68**, 8386–8391.

Couderc, T., Delpeyroux, F., Le Blay, H. & Blondel, B. (1996). Mouse adaptation determinants of poliovirus type 1 enhance viral uncoating. *J Virol* **70**, 305–312.

Gualano, R. C., Pryor, M. J., Cauchi, M. R., Wright, P. J. & Davidson, A. D. (1998). Identification of a major determinant of mouse neurovirulence of dengue virus type 2 using stably cloned genomic-length cDNA. *J Gen Virol* **79**, 437–446.

Hashimoto, I. & Hagiwara, A. (1982). Pathogenicity of a poliomyelitis-like disease in monkeys infected orally with enterovirus 71: a model for human infection. *Neuropathol Appl Neurobiol* **8**, 149–156.

Hashimoto, I., Hagiwara, A. & Kodama, H. (1978). Neurovirulence in cynomolgus monkeys of enterovirus 71 isolated from a patient with hand, foot and mouth disease. *Arch Virol* **56**, 257–261.

Hogle, J. M., Chow, M. & Filman, D. J. (1985). Three-dimensional structure of poliovirus at 2.9Å resolution. *Science* **229**, 1358–1365.

Jia, Q., Hogle, J. M., Hashikawa, T. & Nomoto, A. (2001). Molecular genetic analysis of revertants from a poliovirus mutant that is specifically adapted to the mouse spinal cord. *J Virol* **75**, 11766–11772.

Li, J. P. & Baltimore, D. (1990). An intragenic revertant of a poliovirus 2C mutant has an uncoating defect. *J Virol* **64**, 1102–1107.

Lum, L. C., Wong, K. T., Lam, S. K., Chua, K. B., Goh, A. Y., Lim, W. L., Ong, B. B., Paul, G., AbuBakar, S. & Lambert, M. (1998). Fatal enterovirus 71 encephalomyelitis. *J Pediatr* **133**, 795–798.

Martin, A., Wychowski, S., Couderc, T., Crainic, R., Hogle, J. & Girard, M. (1988). Engineering a poliovirus type 2 antigenic site on a type 1 capsid results in a chimeric virus which is neurovirulent for mice. *EMBO J* **7**, 2839–2847.

Martin, A., Benichou, D., Couderc, T., Hogle, J., Wychowski, S. & Girard, M. (1991). Use of a type 1/type 2 chimeric poliovirus to study determinants of poliovirus type 1 neurovirulence in a mouse model. *Virology* **180**, 648–658.

McMinn, P. C. (2002). An overview of the evolution of enterovirus 71 and its clinical and public health significance. *FEMS Microbiol Rev* **26**, 91–107.

McMinn, P., Stratov, I., Nagarajan, L. & Davis, S. (2001a). Neurological manifestations of enterovirus 71 infection in children during an outbreak of hand, foot, and mouth disease in Western Australia. *Clin Infect Dis* **32**, 236–242.

McMinn, P. C., Lindsay, K., Perera, D., Chan, H. M., Chan, K. P. & Cardosa, M. J. (2001b). Phylogenetic analysis of enterovirus 71 strains isolated during linked epidemics in Malaysia, Singapore and Western Australia. *J Virol* **75**, 7732–7738.

Pfister, T. & Wimmer, E. (1999). Characterization of the nucleoside triphosphatase activity of poliovirus protein 2C reveals a mechanism by which guanidine inhibits poliovirus replication. *J Biol Chem* **274**, 6992–7001.

Reed, L. J. & Muench, H. (1938). A simple method of estimating fifty percent endpoints. *Am J Hyg* **27**, 493–497.

Schmidt, N. J., Lennette, E. H. & Ho, H. H. (1974). An apparently new enterovirus isolated from patients with disease of the central nervous system. *J Infect Dis* **129**, 304–309.

Stanway, G., Brown, F., Christian, P., Hovi, T., Hyypiä, T., King, A. M. Q., Knowles, N. J., Lemon, S. M., Minor, P. D. & other authors(2005). Family *Picornaviridae*. In *Virus Taxonomy. Eighth Report of the International Committee on Taxonomy of Viruses*, pp. 757–778. Edited by C. M. Fauquet, M. A. Mayo, J. Maniloff, U. Desselberger & L. A. Ball. San Diego: Elsevier Academic Press.

Teterina, N. L., Egger, D., Bienz, K., Brown, D. M., Semler, B. L. & Ehrenfeld, E. (2001). Requirements for assembly of poliovirus replication complexes and negative-strand RNA synthesis. *J Virol* **75**, 3841–3850.

Vance, L. M., Moscufo, N., Chow, M. & Heinz, B. A. (1997). Poliovirus 2C region functions during encapsidation of viral RNA. *J Virol* **71**, 8759–8765.

Wang, Y. F., Chou, C. T., Lei, H. Y., Liu, C. C., Wang, S. M., Yan, J. J., Su, I. J., Wang, J. R., Yeh, T. M. & other authors (2004). A mouse-adapted enterovirus 71 strain causes neurological disease in mice after oral infection. *J Virol* **78**, 7916–7924.

Wien, M. W., Curry, S., Filman, D. J. & Hogle, J. M. (1997). Structural studies of poliovirus mutants that overcome receptor defects. *Nat Struct Biol* **4**,666–674.

Wright, A. J. & Phillpotts, R. J. (1998). Humane endpoints are an objective measure of morbidity in Venezuelan encephalomyelitis virus infection of mice. *Arch Virol* **143**, 1155–1162.